Journal of Computational and Applied Mathematics 259 (2014) 805–814

Contents lists available at ScienceDirect

Journal of Computational and Applied Mathematics

journal homepage: www.elsevier.com/locate/cam

A numerical method for imaging of biological microstructures by VHF waves

Guido Ala [a], Pietro Cassarà [b], Elisa Francomano [c,*], Salvatore Ganci [a], Giuseppe Caruso [d], Pio D. Gallo [e]

[a] Università degli Studi di Palermo, DEIM, Palermo, Italy
[b] CNR, Istituto di Scienza e Tecnologie dell'Innovazione, Pisa, Italy
[c] Università degli Studi di Palermo, DICGIM, Palermo, Italy
[d] Università degli Studi di Palermo, DIBIMEF, Palermo, Italy
[e] Università degli Studi di Palermo, DICHIRONS, Palermo, Italy

ARTICLE INFO

Article history:
Received 13 February 2013
Received in revised form 11 June 2013

Keywords:
Method of Moments
Non-linear model
Inverse problem
Levenberg–Marquardt method
Biological microstructures
Non ionizing waves

ABSTRACT

Imaging techniques give a fundamental support to medical diagnostics during the pathology discovery as well as for the characterization of bio-medical structures. The imaging methods involve electromagnetic waves in a frequency range that spans from some Hz to GHz and over. Most of these methods involve ionizing waves and scanning of a large human body area even if only a focused inspection is needed. In this paper, a numerical method to evaluate the shape of microstructures for application in the medical field, with a very low invasiveness for the human body, is proposed. In particular, the tooth's root canal is considered. In fact, this is one of the hot topics in the endodontic procedures where rotary instruments are widely used. These instruments are subjected to sudden mechanical damage during the surgical process, due to cyclic fatigue directly related to the canal's geometrical characteristics. In order to develop an improved endodontic procedure so that instrument breakage probability and canal milling precision are optimized, preliminary canal root reconstruction techniques have to be implemented. These techniques are usually based on invasive X-ray imaging. Thus, a minimally invasive, easy to use imaging technique that can be applied many times on the patient is of great interest. To this aim, a method based on a flexible thin-wire antenna radiating non ionizing VHF waves is proposed. By measuring the spatial magnetic field distribution in the neighboring area, it is possible to reconstruct the microstructure image by estimating the shape of the antenna against a sensor panel. The mathematical model is strictly non-linear and the inverse problem described above is solved numerically; first simulation results are presented in order to show the validity and the robustness of the proposed approach.

1. Introduction

The support given by imaging techniques to medical diagnostics is fundamental during the pathology discovery as well as for characterization of biological structures [1–7]. The imaging methods involve electromagnetic waves in a frequency range that spans from some Hz to GHz and over. Hence, the understanding of biological structure response to the electromagnetic field is fundamental. The investigation of the interaction between healthy or pathological biological tissues and

* Corresponding author.
E-mail address: elisa.francomano@unipa.it (E. Francomano).

0377-0427/$ – see front matter © 2013 Elsevier B.V. All rights reserved.
http://dx.doi.org/10.1016/j.cam.2013.07.020

electromagnetic waves is still a hot topic [8]. In fact,understanding how an electromagnetic wave interacts with the human body becomes increasingly important if one considers that the most of imaging methods involve the scanning of wide areas of the human body, even if only a focused inspection is needed. In this way, although a wide scanning allows the acquisition of a big amount of data by single exposition, also areas of the body not interested in the diagnostics are exposed to the waves, so increasing the invasiveness for the patient. For this reason, new imaging systems able to analyze only a focused area (confined scanning), are becoming more and more investigated [5]. A big input to micro-imaging systems has been given by micro-electronic technology, which allows the development of systems for scanning of confined small areas. In fact, emitters and receivers (sensors) can be made smaller and smaller, so that the final size of the imaging systems as well as the wave spots become very small. Generally, the acquired data need to be appropriately elaborated extracting the imaging information by means of inverse optimization algorithms [3,4,7]. Through these algorithms high quality information can be extracted from the data acquired by the sensors, even if the quality of the sensors signal is low. In this paper a method for the shape recognition of microstructures with application in medical field is proposed. Precisely, the tooth's root canal reconstruction is considered. In fact, this is one of the hot topics in the endodontic field where rotary instruments are widely used. These instruments, named files, used for surgical procedures, are subjected to various types of mechanical stress, directly related to canal's characteristics. In particular, file separation caused by cyclic fatigue is still an unsolved problem. Moreover, it occurs without warning since no indication of plastic deformation appears during the surgical process. Cyclic fatigue studies, often supported by file builders, have shown the influence of canal shape (i.e. angle, curvature radius, length, possible bifurcations) on mechanical stresses, so deeply modifying the instrument life and, consequently, its breakage [9,10]. In order to develop an improved endodontic procedure through which the breakage probability of the files and milling precision of the canal are optimized, root canal reconstruction techniques have to be implemented. These techniques are usually based on invasive X-ray imaging: in fact, for most of the endodontic procedures this imaging technique has to be performed many times, so exposing the patient to an unwanted X-ray dose amount. Moreover, the effective canal shape reconstruction remains a critical task [9,10].

Hence, an imaging method which is easy to use, with low invasiveness, with a satisfactory precision, and that can be applied many times on the patient, can become a fundamental task for these applications.

The proposed method works with non ionizing low power electromagnetic waves, in the Very High Frequency (VHF) range, in order to achieve a low level of invasiveness for the human body. The method uses a system endowed with a microtransmitter, a sensor panel to acquire the spatial distribution of the electromagnetic field in the close proximity and an elaboration logic to acquire and elaborate the sensors signals. The micro transmitter radiates the VHF waves by means of a flexible thin-wire microantenna, inserted in the root canal. Hence, the micro antenna can be assumed to have the same shape of the analyzed structure. By measuring the spatial distribution of the magnetic field in the neighborhood of the thin-wire antenna, it is possible to reconstruct the microstructure image. In fact, the shape reconstruction is possible by estimating the location of thin-wire antenna against the sensor panel. The recognition problem of the thin-wire antenna location by magnetic field measurements can be addressed as an inverse problem. The thin-wire antenna is supposed to be a sequence of linear segments: given a model for the characterization of the magnetic field at a set of points in space (forward problem) and given a set of measurements at these points, it is possible to solve the inverse problem in terms of the distances of the antenna axis points from the sensor panel. The magnetic field component is selected since the physical domain can be characterized with a uniform magnetic permeability in the VHF range. In this paper, first results about the previous idea are reported concerning two simulated scenarios. Namely, the spatial distribution of the emitted magnetic field is simulated through a numerical model based on the method of moments (MoM), where the first kind Fredholm integral equation is solved by the point matching procedure [11–17]. The field values are used as the measured input for the inverse problem. The Levenberg–Marquardt algorithm [18,19] is used in solving the inverse problem by means of minimization of the Euclidean distance between the measured field and the field generated by a given configuration of thin-wire piecewise antenna. The numerical procedure involved by the algorithm rounds the entries of the Hessian matrix, step by step, and the location of the antenna segments can be estimated with satisfactory precision, so obtaining the image of the canal shape.

The paper is structured as follows. In Section 2 the mathematical framework about the proposed method is presented. In Section 3 numerical results about reconstruction examples are discussed, then a conclusion about results and ongoing work completes the paper.

2. Numerical approach

The biological thin microstructures taken into account in this paper are shown in Fig. 1. The Figure shows the typical shape of a root canal: in this case the canal reveals two curvature changes along the whole length. As already underlined, due to an inaccurate prediction of these curvature changes, the endodontic files suffer from mechanical stress that can cause unwanted breakage and added problems in the patient. The shape of these microstructures can be estimated by means of an appropriate embedded emitting antenna and by measuring the spatial distribution of the appropriate radiated electromagnetic field component. In particular, the magnetic field may be the best choice together with the selection of the appropriate work frequency range. The proposed approach is a typical inverse problem: the measured spatial distribution of the magnetic field emitted by a VHF thin-wire antenna (i.e. with radius less than one hundredth of the maximum work wavelength) is the input, and the source shape reconstruction is the final target. The antenna is assumed to be a piecewise linear structure, i.e. a sequence of N_b branches with uniform radius r_c and conductivity σ_c. The antenna is fed at the point (x_0, y_0, z_0)

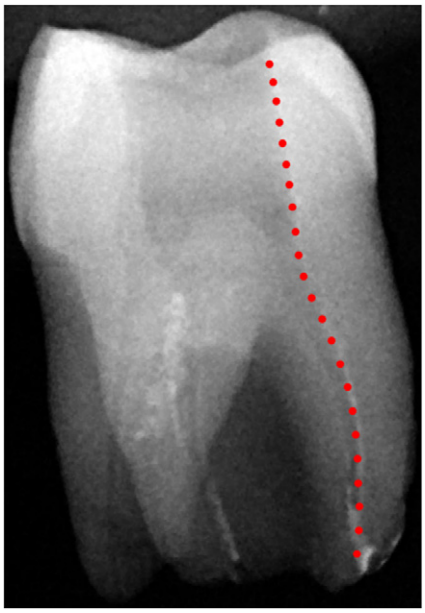

Fig. 1. Tooth's root canal (point red line). (For interpretation of the references to colour in this figure legend, the reader is referred to the web version of this article.)

by a sinusoidal current source with known frequency f and amplitude I_{source}. The spatial distribution of the magnetic field is detected by a sensor panel with M sensors distributed on its surface. As a first approximation, the surrounding medium is supposed to be homogeneous and isotropic, with conductivity σ, electric permittivity ϵ and magnetic permeability μ. Under these assumptions, the shape reconstruction involves the minimization of an objective function shown in Eq. (1), by using an iterative procedure. Roughly speaking, step by step the iterative procedure looks for a set of segments coordinates that minimize the 2-norm difference between the computed and measured magnetic field at sensor points, i.e. the error function F:

$$\min_{\mathbf{p}}\{F\} = \min_{\mathbf{p}}\left\{\|H_{comp}(\mathbf{p}) - H_{meas}\|_2\right\} \tag{1}$$

In Eq. (1), $\mathbf{p} = [(x_1, y_1, z_1)\cdots(x_{N_b}, y_{N_b}, z_{N_b})]^T$ is the vector of the Cartesian coordinates of the antenna segments ends to be estimated, H_{comp} is the vector of the magnetic field values at sensor points computed by assuming that the segments ends are located at $\mathbf{p}$, and H_{meas} is the vector with the measured magnetic field values. The values of H_{comp} are calculated by the forward solver for a given signal source and antenna characteristics. More precisely, the current distribution along the antenna is evaluated by solving an appropriate integral equation in frequency domain, derived from Maxwell equations. Then, by using the relation that links the currents to the magnetic field, the latter can be calculated at the sensor points. The equations of the forward model are solved numerically. For the problem addressed in this case, the MoM via point-matching procedure in the frequency domain, is performed. Note that, by this method the involved integral equation includes the boundary conditions, so that only the emitter has to be discretized but not the whole problem domain. This means that each antenna branch needs to be split into a finite number of linear segments [11–16]. The problem formulation leads to a first kind Fredholm integral equation. In fact, by expressing the electric field $\vec{E}$ with the retarded magnetic vector potential $\vec{A}$, the source frequency ($\omega = 2\pi f$) and the scalar electric potential ϕ, as shown in Eq. (2):

$$\vec{E} = -(\nabla\phi + j\omega\vec{A}) \tag{2}$$

and by introducing the boundary conditions by means of the per-unit-length surface impedance $\dot{z_s}$, the following equation holds:

$$\begin{aligned} &\vec{u}\cdot\vec{E} = \dot{z_s}I_s \\ &-(\nabla\phi + j\omega\vec{A})_{tg} = z_sI_s \end{aligned} \tag{3}$$

in which the subscript tg indicates the component tangential to the wire surface, I_s is the longitudinal current flowing into the conductor, supposed concentrated on its axis ($\vec{u}'$ as the unit vector) because of the thin-wire assumption [11,14], $\vec{u}$ is the unit vector tangential to the conductor's surface, as shown in Fig. 2.

By using the relation between the magnetic vector potential $\vec{A}$ and the conduction current density, and the relation between the scalar electric potential ϕ and the free electric charge density, the well known electric field integral equation

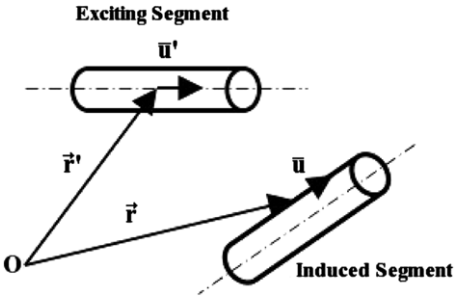

Fig. 2. General thin-wire geometric references.

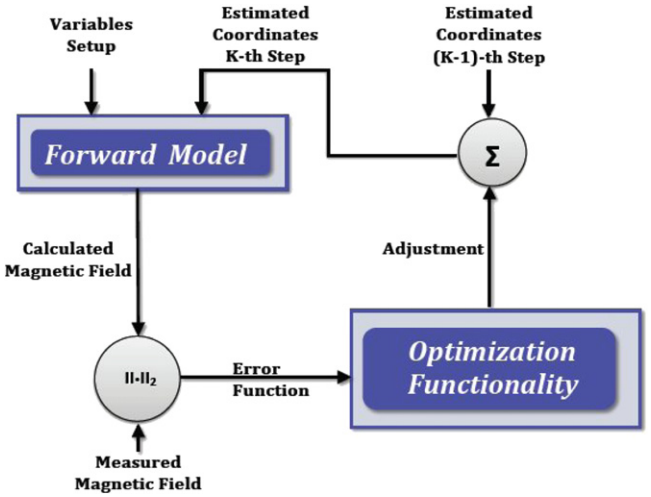

Fig. 3. Blocks diagram of the inverse problem algorithm. (For interpretation of the references to colour in this figure legend, the reader is referred to the web version of this article.)

(EFIE) is obtained. Then, by integrating the EFIE along the surface of the conductor, the following modified EFIE is obtained [11,14]:

$$j\omega \int_L \vec{u} \cdot \int_\Omega \mu I_s(l') g(\vec{r}, \vec{r}') dl' dl + \int_L \frac{\partial}{\partial l_{tg}} \frac{1}{j\omega\dot{\epsilon}} \int_\Omega \frac{dI_s(l')}{dl'} g(\vec{r}, \vec{r}') dl' dl = -\dot{z}_s \int_L I_s(\vec{r}) dl. \tag{4}$$

Eq. (4) is a general relation that depends only on the longitudinal current and on geometrical quantities related to the conductors constituting the thin-wire structures to be analyzed. In fact, Ω is the length of the exciting conductor, L is the length of the induced conductor, $\vec{r}$ and $\vec{r}'$ are space position vectors of the observation and source points, respectively; $g(\vec{r}, \vec{r}') = \frac{e^{-k|\vec{r}-\vec{r}'|}}{4\pi|\vec{r}-\vec{r}'|}$ is the Green's function in an unbounded region. The quantity $\dot{\epsilon} = \epsilon + j\omega\sigma$ takes into account the complex medium permittivity and $\dot{k} = \sqrt{-\omega^2\mu\dot{\epsilon}}$ is the wave number. As already underlined, the forward problem, represented by Eq. (4), is numerically solved by splitting the thin-wire antenna into a finite number of linear segments of length δ. In scientific literature numerous results [11,14] show that an acceptable accuracy can be obtained for the solution of Eq. (4), by assuming $\delta \leq 0.05\lambda$ and a spatial linear distribution of current along the axis of each segment. In this way, a linear system of order $n + N_b$ is obtained with n as the number of segments. Once the currents are computed, the magnetic field components in the surrounding medium are given by the dipole theory, by superposing the effects of all segments [11,14]. As discussed above, once the direct problem is solved, the inverse one can be then approached. In Fig. 3 a block diagram for the algorithm used to solve the inverse problem is shown. The unknown end-point segment coordinates $\mathbf{p}$ are obtained through an iterative procedure which, at each step, computes the correction factors needed to obtain the new set of points coordinates. The correction factors are evaluated by the optimization functionality, on the basis of the difference in 2-norm among the measured fields and the fields computed by the forward solver. Since the problem is strictly nonlinear, the inverse problem solver is based on the Levenberg–Marquardt (LM) algorithm [18]. In brief, the LM algorithm starts from an initial set of reasonable end-point segment coordinates $\mathbf{p}^{(0)}$: this set is then updated at each step k by adding the solutions $\Delta\mathbf{p}^{(k)}$ of the linear system shown in Eq. (5):

$$\left(\tilde{\mathbf{B}}^{(k)} + \beta^{(k)} \mathrm{diag}[\tilde{\mathbf{B}}^{(k)}]\right) \Delta\mathbf{p}^{(k)} = -\mathbf{G}^{(k)^T} F(\mathbf{p}^{(k)}) \tag{5}$$

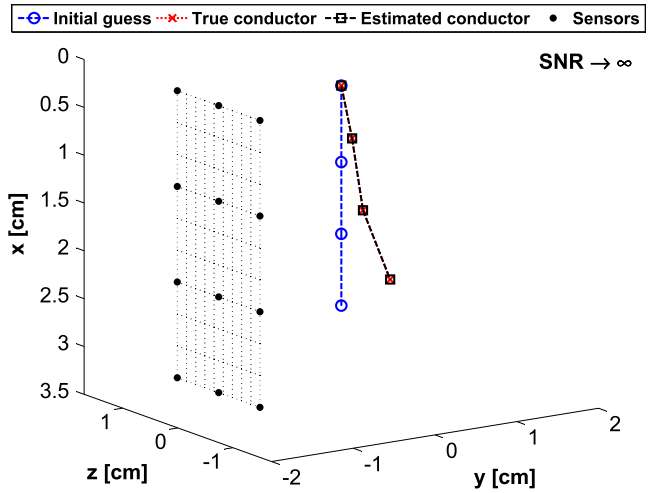

(a) Flat sensor panel.

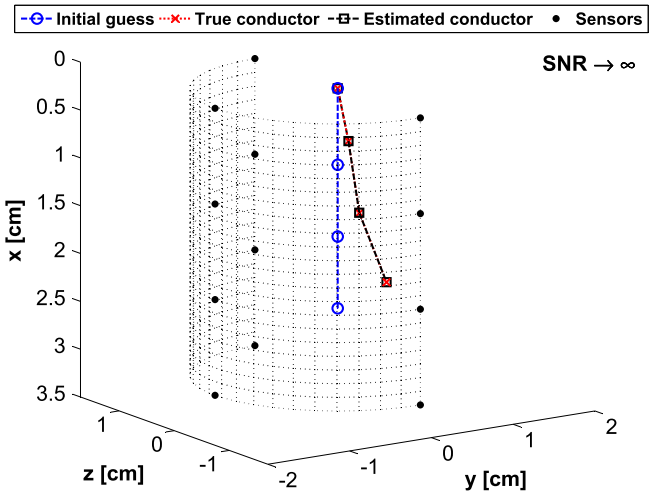

(b) Semi-cylindrical sensor panel.

Fig. 4. Noiseless shape reconstructions. The initial position is that a of straight thin-wire antenna 2.3 cm in length and perpendicular to the Y–Z plane. (For interpretation of the references to colour in this figure legend, the reader is referred to the web version of this article.)

where the matrix $\tilde{\mathbf{B}}^{(k)}$ is an approximation of the Hessian matrix of F at step k and is equal to $\mathbf{G}^{(k)^T}\mathbf{G}^{(k)}$, with $\mathbf{G}^{(k)}$ as the gradient of the error function F at step k, while $\beta^{(k)}$ is an adaptive parameter. Once $\mathbf{\Delta p}^{(k)}$ is known, the new coordinates are calculated by the following relation:

$$\mathbf{p}^{(k+1)} = \mathbf{p}^{(k)} + \Delta\mathbf{p}^{(k)}. \tag{6}$$

3. Numerical results

In order to validate the capabilities of the proposed method, some numerical experiments concerning the shape estimation of a specific tooth's root canal have been carried out.

A NiTi (electrical conductivity $1.1 \cdot 10^6$ S/m) thin-wire antenna 0.1 mm in radius and 2.3 cm in length is assumed to be inserted in the root canal and fed by a sinusoidal current source with frequency equal to 100 MHz. The NiTi alloy is selected because it is commonly used in biomedical applications [9,10]. The antenna shape, which is approximately the canal shape, is shown in Fig. 4(a) and (b) (red dashed line with cross markers). The same figures show also that the ground surface of the antenna lies on the Y–Z plane, and the feed point is placed at a distance of 2 mm from the ground plane. The sensors are assumed to be sensitive to the component of the magnetic field along the Z axis.

In order to approximate the characteristics of a tooth, the medium around the canal is assumed to have zero electrical conductivity, relative permittivity equal to 15 and relative permeability equal to 1 [20].

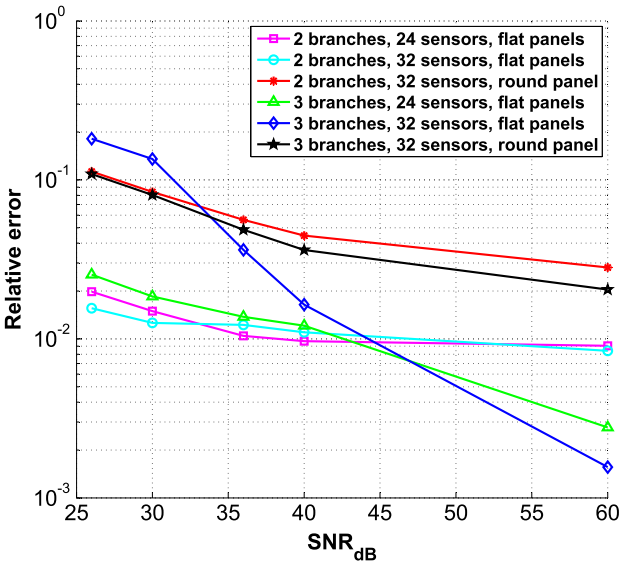

Fig. 5. Relative reconstruction error vs. SNR (dB). (For interpretation of the references to colour in this figure legend, the reader is referred to the web version of this article.)

Two sets of simulations have been carried out: one set concerning a noiseless environment, and one set to test the influence of noise on the shape reconstruction.

In the noiseless context, the Signal to Noise Ratio (SNR) is assumed to approach infinity: the measured values of magnetic field have been calculated by means of the MoM-based forward solver described in Section 2. Different current source amplitudes have been tested: 0.1 mA, 1 mA, 5 mA, 25 mA and 50 mA. It has to be underlined that all these current values as well as the selected frequency, can be well tolerated by the human tissues also depending on the time of application (i.e. a few seconds) [21,8,22,23]. On the other hand, the VHF waves are non ionizing ones with respect to the commonly used X-ray.

Two sets of 12 sensors are considered. The sensors are placed on a flat surface in a first case study (Fig. 4(a)) and on a semi-cylindrical surface in a second case study (Fig. 4(b)). The flat sensor panel is 3 cm in height and 1.5 cm in width, while the semi-cylindrical one is 1.5 cm in radius and 3 cm in height.

The antenna shape has been reconstructed by means of a three branch conductor. The initial set of end-point segment coordinates $\mathbf{p}^{(0)}$ for the LM optimization algorithm is that of a straight thin-wire antenna 2.3 cm in length and perpendicular to the ground plane. From these coordinates the true position of each branch is then estimated.

The estimated conductor position in the flat sensor panel case is shown in Fig. 4(a). In this first noiseless case study, the distance between the estimated shape (black dashed line with square markers) and the true position (the red dashed line with cross markers) is close to zero.

For this configuration, the 2-norm relative error between true and estimated coordinates values for a given current level, and the number of iterations are reported in Table 1. The results show that the error is close to zero, also for small values of the source current.

Fig. 4(b) shows the estimated position of the conductor for the semi-cylindrical sensor panel. For this scenario, the 2-norm relative error between true and estimated coordinates for a given level of source current, and the number of iterations are shown in Table 2. The simulations results show that the error is close to zero also in this case.

The second set of experiments is aimed at studying the influence of noise on reconstruction accuracy.

The measurements are supposed to be affected by additive white Gaussian noise: the measured values of magnetic field have been calculated by means of the MoM-based forward solver described in Section 2 and then the noise has been added.

Our experiments showed that the sensor panels tested in the ideal noiseless case are not able to provide an acceptable reconstruction accuracy in a noisy environment. Therefore more complex sensor panels has been tested, namely 24 or 32 sensors on two parallel flat panels (each panel is 3 cm in height and 1.5 cm in width, see Figs. 6 and 7 respectively) and 32 sensors on a cylindrical panel (1.5 cm in radius and 3 cm in height, see Fig. 8).

Moreover, in order to test the effect of an increasing number of variables involved in the optimization process on reconstruction accuracy, the shape of the antenna has been reconstructed by assuming a two branch conductor or a three branch conductor, alternatively: if one considers common canal shapes and curvatures, both of these configurations can potentially represent the canal shape in a satisfactory way.

The behavior of the relative reconstruction error versus the SNR for different sensor panels and numbers of assumed antenna branches is shown in Fig. 5. In Figs. 6–8, some reconstructions are also shown for low values of SNR. In all these experiments, the current source amplitude has been set to 50 mA.

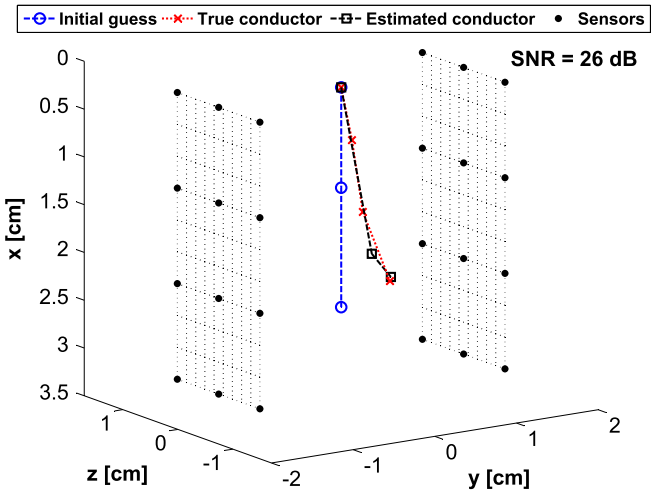

(a) Two segments.

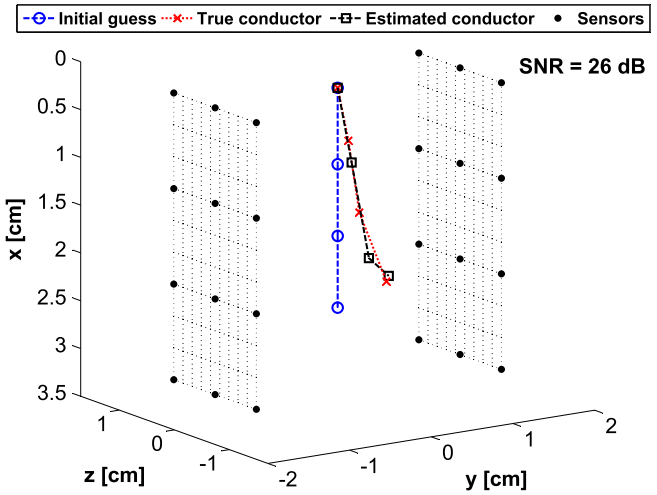

(b) Three segments.

Fig. 6. Shape reconstruction in noisy environment, two flat sensor panels (24 sensors). (For interpretation of the references to colour in this figure legend, the reader is referred to the web version of this article.)

Table 1
Relative error and number of iterations required with the flat sensor panel.

Current (mA)	Relative error	No. of iterations
0.1	6.15e−11	169
1	6.10e−11	165
5	7.88e−09	87
25	3.78e−10	28
50	1.53e−11	8

Table 2
Relative error and number of iterations required with the semi-cylindrical sensor panel.

Current (mA)	Relative error	No. of iterations
0.1	3.05e−10	25
1	1.04e−09	17
5	1.75e−11	12
25	2.55e−12	8
50	1.00e−09	8

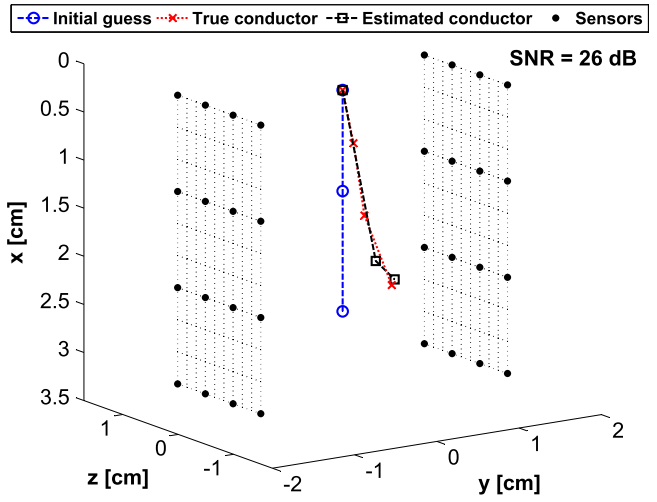

(a) Two segments.

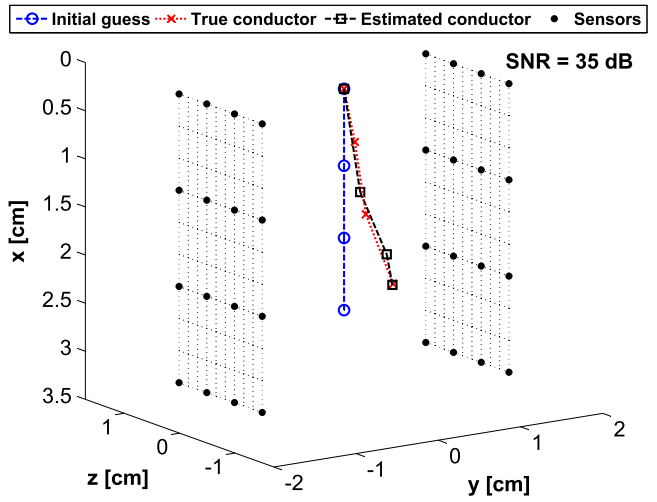

(b) Three segments.

Fig. 7. Shape reconstruction in noisy environment, two flat sensor panels (32 sensors). (For interpretation of the references to colour in this figure legend, the reader is referred to the web version of this article.)

It turns out that satisfactory accuracies can be achieved with all the configurations tested, even when the SNR is low. However, by approximating the antenna with a two branch conductor, a better robustness with respect to noise can be achieved, without compromising accuracy. In particular, two branch conductors reconstructions outperform three branch ones for very noisy environments. In general, for a fixed number of conductor branches, the best results are obtained by employing flat sensor panels.

4. Conclusions

In this paper, a numerical approach to reconstruct the shape of microstructures for bio-medical application with a very low invasiveness for the human body, is proposed. The tooth's root canal reconstruction is considered. This is one of the hot topics in endodontic procedures where there is a wide use of rotary instruments (files) subjected to various types of mechanical stress, directly related to the canal's characteristics. File separation, caused by cyclic fatigue, occurs without warning, so determining unwanted failure of the endodontic procedure, also with potential surgery complication for the patient. Therefore, preliminary root canal reconstruction techniques have to be implemented in order to optimize the endodontic procedure. These techniques are usually based on invasive X-ray imaging. In fact, for most of the endodontic procedures this imaging technique has to be performed many times, so exposing the patient to an unwanted X-ray dose amount. Moreover, the effective canal shape reconstruction remains a critical task. In the paper, a minimally invasive, easy to use imaging technique that can be applied many times on the patient, is proposed. It is based on a flexible thin-wire

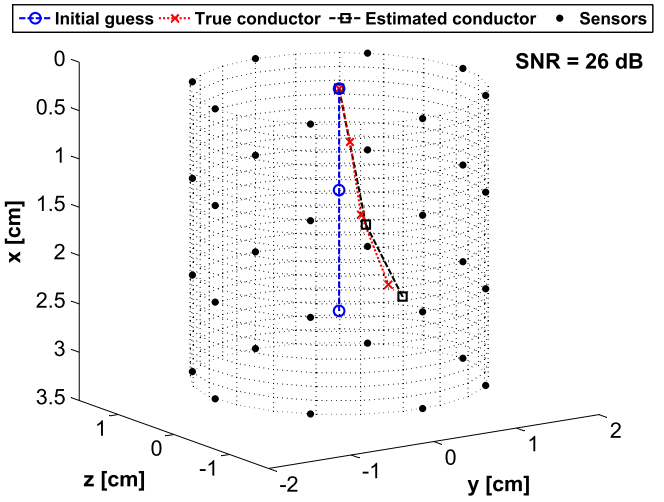

(a) Two segments.

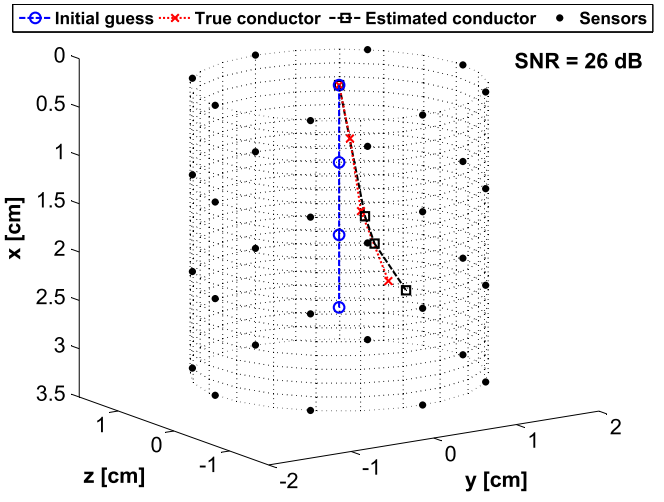

(b) Three segments.

Fig. 8. Shape reconstruction in noisy environment, cylindrical sensor panel (32 sensors). (For interpretation of the references to colour in this figure legend, the reader is referred to the web version of this article.)

antenna radiating non ionizing VHF waves and inserted in the canal. The typical inverse problem is solved numerically: the estimation of the antenna shape enables the reconstruction of the canal image with a satisfactory approximation. The first simulation results also show the validity and the robustness of the proposed approach. A prototype of the actual application is currently under construction.

Acknowledgment

This work has been supported by University of Palermo, under FFR2012 research project.

References

[1] G. Ala, G. Di Blasi, E. Francomano, Numerical meshless particle method in solving the magnetoencefalography forward problem, International Journal of Numerical Modeling: Electronic Networks, Devices and Fields 25 (5–6) (2012) 428.
[2] G. Ala, E. Francomano, Multi-sphere particle numerical model for non-invasive investigations of neuronal human brain activity, Progress In Electromagnetic Research Letters 36 (2013) 143–153.
[3] P. Di Barba, M.E. Mognaschi, G. Nolte, R. Palka, A. Savini, Source identification based on regularization and evolutionary computing in biomagnetism, The International Journal for Computation and Mathematics in Electrical and Electronic Engineering 29 (4) (2010) 1022–1032.
[4] A. Fhager, P. Hashemzadeh, M. Persson, Reconstruction quality and spectral content of an electromagnetic time-domain inversion algorithm, IEEE Transactions on Biomedical Engineering 53 (8) (2006) 1594–1604.

[5] R.D. Foster, D.A. Pistenmaa, T.D. Solberg, Comparison of radiographic techniques and electromagnetic transponders for localization of the prostate, Radiation Oncology 7 (1) (2012).
[6] Z. Zakaria, R.A. Rahim, M.S.B. Mansor, S. Yaacob, N.M.N. Ayob, S.Z.M. Muji, M.H.F. Rahiman, S.M.K.S. Aman, Advancements in transmitters and sensors for biological tissue imaging in magnetic induction tomography, Sensors 12 (6) (2012) 7126–7156.
[7] T. Williams, J. Sill, E. Fear, Breast surface estimation for radar based breast imaging systems, IEEE Transactions on Biomedical Engineering 55 (6) (2008) 1678–1686.
[8] D.B. Davidson, U. Jakobus, M.A. Stuchly, Human exposure assessment in the near field of gsm base-station antennas using a hybrid finite element/method of moments technique, IEEE Transactions on Biomedical Engineering 50 (2) (2003) 224–233.
[9] D. Sonntag, S. Stachniss-Carp, C. Stachniss, V. Stachniss, Determination of root canal curvatures before and after canal preparation (part ii): a method based on numeric calculus, Journal Compilation Australian Society of Endodontology 32 (2006) 16–25.
[10] J. Wan, B.J. Rasimick, B.L Musikant, A.S. Deutsch, A comparison of cyclic fatigue resistance in reciprocating and rotary nickel-titanium instruments, Journal Compilation Australian Society of Endodontology 37 (2011) 122–127.
[11] G. Ala, P. Buccheri, E. Francomano, A. Tortorici, Advanced algorithm for transient analysis of grounding systems by moments method, in: IEE, editor, IEE Conference Publication, 1994, pp. 363–366.
[12] G. Ala, E. Francomano, A. Tortorici, Iterative moment method for electromagnetic transients in grounding systems on cray t3d, Lecture Notes in Comput. Sci. 1041 (1) (1996) 9–16.
[13] G. Ala, E. Francomano, A. Tortorici, The method of moments for electromagnetic transients in grounding systems on distributed memory multiprocessors, Parallel Algorithms and Applications 14 (3) (2000) 213–233.
[14] G. Ala, M.L. Di Silvestre, Simulation model for electromagnetic transients in lightning protection systems, IEEE Transactions on Electromagnetic Compatibility 44 (4) (2002) 539–554.
[15] G. Ala, M.L. Di Silvestre, E. Francomano, A. Tortorici, Advanced numerical model in solving thin-wire integral equations by using semi-orthogonal compactly supported spline wavelets, IEEE Transactions on Electromagnetic Compatibility 45 (2) (2003) 218–228.
[16] G. Ala, M.L. Di Silvestre, E. Francomano, A. Tortorici, Wavelet-based efficient simulation of electromagnetic transients in a lightning protection system, IEEE Transactions on Magnetics 39 (3) (2003) 1257–1260.
[17] G. Ala, M.C. Di Piazza, G. Tine, F. Viola, G. Vitale, Evaluation of radiated emi in 42 v vehicle electrical systems by fdtd simulation, IEEE Transactions on Vehicular Technology 56 (4) (2007) 1477–1484.
[18] W.H. Press, S.A. Teukolsky, W.T. Vetterling, B.P. Flannery, Numerical Recipes: The Art of Scientific Computing, Cambridge University Press, Cambridge, 2007.
[19] E. Francomano, A. Tortorici, C. Lodato, S. Lopes, An algorithm for optical flow computation based on a quasi-interpolant operator, Computing Letters 2 (1–2) (2006) 93–106.
[20] C. Gabriel, Compilation of the dielectric properties of body tissues at rf and microwave frequencies, in: Technical Report AUOE-TR-1996-0037, Physics Department, King's College, London WC2R2LS, UK, 1996.
[21] A. Barth, I. Ponocny, T. Gnambs, R. Winker, No effects of short-term exposure to mobile phone electromagnetic fields on human cognitive performance: a meta-analysis, Bioelectromagnetics 33 (2) (2012) 159–165.
[22] R.P. O'Connor, S.D. Madison, P. Leveque, H.L. Roderick, M.D. Bootman, Exposure to gsm rf fields does not affect calcium homeostasis in human endothelial cells, rat pheocromocytoma cells or rat hippocampal neurons, PLoS One 5 (7) (2010) 1–16.
[23] F. Sibella, M. Parazzini, A. Paglialonga, P. Ravazzani, Assessment of sar in the tissues near a cochlear implant exposed to radio frequency electromagnetic fields, Physics in Medicine and Biology 54 (8) (2009) 135–141.